

Journal of Materials Chemistry A

Accepted Manuscript



This is an *Accepted Manuscript*, which has been through the Royal Society of Chemistry peer review process and has been accepted for publication.

Accepted Manuscripts are published online shortly after acceptance, before technical editing, formatting and proof reading. Using this free service, authors can make their results available to the community, in citable form, before we publish the edited article. We will replace this *Accepted Manuscript* with the edited and formatted *Advance Article* as soon as it is available.

You can find more information about *Accepted Manuscripts* in the [Information for Authors](#).

Please note that technical editing may introduce minor changes to the text and/or graphics, which may alter content. The journal's standard [Terms & Conditions](#) and the [Ethical guidelines](#) still apply. In no event shall the Royal Society of Chemistry be held responsible for any errors or omissions in this *Accepted Manuscript* or any consequences arising from the use of any information it contains.

Atomistic molecular dynamics simulations reveal insights into adsorption, packing, and fluxes of molecules with carbon nanotubes.

*Matteo Calvaresi, * Francesco Zerbetto**

Dipartimento di Chimica “G. Ciamician”, Alma Mater Studiorum - Università di Bologna, via F. Selmi, 2 - 40126 Bologna, Italy

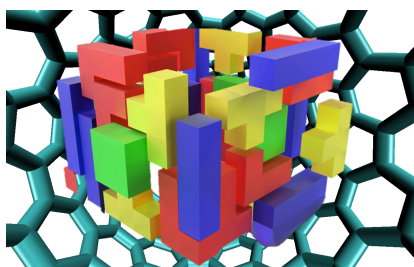
E-mail: matteo.calvaresi3@unibo.it, francesco.zerbetto@unibo.it



Matteo Calvaresi was born in 1979 and received his Ph.D. in 2008. In 2011, he became Assistant Professor of Organic Chemistry at the University of Bologna. He was Visiting Researcher at Peking University, China, and Visiting Professor at University of Pune, India. His current research interests focus on the study of interactions between molecules and biomolecules with carbon nanomaterials, both experimentally and computationally.



Francesco Zerbetto was born in 1959 and received his Ph.D. in 1986. He was then Research Associate at NRC, Ottawa, until 1990 when he was appointed Researcher at the University of Bologna. He has been Professor of Physical Chemistry since 2001 and serves now as Head of Department. His research, in computational and theoretical chemistry, has covered vibrationally resolved electronic spectroscopies, tunneling effect, nonlinear optics, carbon nanostructures, chirality, interlocked molecules, surface science, and self-assembly.

TOC

Atomistic simulations provide a molecular-level understanding of the basic phenomena that govern molecules/carbon nanotube interactions: adsorption, packing and fluxes.

ABSTRACT

This feature article discusses the current progress and the problems of applications of atomistic simulations to the understanding of the basic phenomena that govern molecules / carbon nanotube (CNT) interactions that bear on gas storage, sustainability and living. Molecular adsorption is assessed in the light of molecular dynamics, MD, simulations that reveal the most favourable adsorption sites of molecules and allow the interpretation of experimental data and the determination of the energy contributions to the binding. Packing is examined in view of calculations for the application of CNT for gas storage and CO₂ capture and removal. Fluxes are discussed for the separation of different types of ions in water, seawater desalination, removal of drinking water contaminants, and gas separation. Difficulties related to the modelling and to possible improvement and upscaling of the calculations are also addressed.

1. INTRODUCTION

The unique and tunable properties of carbon nanotubes (CNTs) have attracted special attention for a wide range of potential applications that cover gas storage, sustainability and living. The foreseen technology covers sorbents, high-flux membranes, molecular-level storage systems, depth filters, antimicrobial agents, environmental and diagnostic sensors.¹ All these technological applications are based on three fundamental processes: adsorption,² packing³ and flux.⁴ This feature article considers a few examples: (i) the adsorption and/or self-assembly of molecules and biomolecules inside/outside a tube² for solid-phase extraction, materials for water treatment and sensing; (ii) packing of molecules inside tubes³ for hydrogen/methane storage and carbon dioxide capture; (iii) flux of molecules inside tubes⁴ for CNTs-based membranes, and CNTs based water desalination treatments.

Despite extensive experimental research, the comprehension of the nature of the interactions of organic and inorganic molecules with CNT surface at the liquid (or gas)/solid interface is still partly elusive. It is very difficult to determine experimentally the (equilibrium) morphology of the molecules/tube interface - which makes it hard to characterize the structure and dynamics of the molecules interacting with the tubes. Atomistic simulations may provide a molecular-level understanding of the fundamental interactions between molecules and CNTs. Molecular dynamics (MD) simulations, in particular, allow the description of molecular adsorption, packing and flux of molecules in precise conditions and, being atomically resolved, give detailed microscopic information. The simulations can determine also information on the kinetics of the phenomena that is the path a system follows in order to reach equilibrium.

This work discusses current progresses and issues related to the applications of MD simulations with the intent of understanding the basic phenomena governed by molecules/CNT interactions that have applications in gas storage, sustainability and living.

2. ADSORPTION

CNTs offer chemically inert surfaces for physical adsorption, with an extremely high surface area to volume ratio (up to 1600 m²/g). In recent years, the adsorption of organic chemicals on CNTs has attracted increasing attention. CNTs have been considered promising materials for solid-phase extraction cartridges, waste water treatment, ground water remediation and molecular and ionization sensors.⁵ Understanding the adsorption mechanisms and determining the affinity of molecules for CNTs is crucial for the improvement of their applications.⁶

Carbon Nanotubes as Sorbents

Molecular dynamics simulations have provided a description of physical and chemical processes that are inaccessible to experimental techniques and are ideally suited for studying the conformational dynamics and adsorption/desorption behaviour of molecules on CNTs.

i) MD simulations can reveal the most favourable adsorption states of molecules on CNTs.

CNTs associate with each other to form bundles that typically comprise tens or hundreds of individual tubes. Adsorption of molecules takes place on these bundles. In order to gain insight into the adsorption on CNTs, it is necessary to consider the structure of the bundle and the available adsorption sites (Figure 1a). Four types of adsorption sites can be identified: (i) nanotube interior sites, (ii) sites on the external surface, (iii) groove sites, and (iv) interstitial sites.²

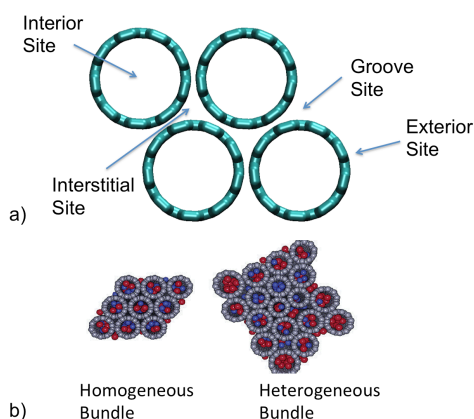


Figure 1. (a) Four types of adsorption sites exist in CNTs bundles. (b) Homogeneous and heterogeneous packing of CNTs determine different adsorbing surfaces. Reprinted with permission from Ref 8. Copyright 2003 American Chemical Society.

The groove sites are narrow troughs formed outside the bundles where two CNTs abut. The interstitial sites are channels between individual CNTs inside the bundle. Simulations showed that CNT interior has the highest binding energy for adsorbing molecules. The presence of the surrounding walls maximizes the attractive van der Waals interactions with the adsorbed molecule. On the other hand, the nanotube external wall curves away from the adsorbed molecules, which implies that the adsorption energy must be smaller than that for the interior or for flat graphene. The adsorption energy for groove sites lies between the adsorption energies of external and internal sites.⁷ Adsorption of molecules in the interstitial channels is a topic still under debate. Molecular simulations shed light on the ongoing controversy. They showed that also small species such as Xe or CF₄ only adsorb inside the nanotubes and on the external grooves of perfectly packed homogeneous bundles (Figure 1b). The interstitial channels, in homogeneous bundles of nanotubes, are too small to allow adsorption of either gas. However, CNTs usually form heterogeneous bundles that do not pack perfectly and have a few larger interstitial sites that potentially fit gas adsorption.^{8,9} The packing of CNTs determines the possibility to have molecules adsorbed in the interstitial channels.

ii) *Simulations allow the interpretation of experimental data*

Atomistic simulations probe molecular-level details of adsorption and can interpret experimental data. For example, three distinct adsorption sites were observed on CNTs for alkane adsorption using temperature-programmed desorption.⁷ Only using atomistic simulations it was possible to assign the sites. Simulations found that desorption from the exterior surface of the nanotubes occurs at the lowest temperature, followed by that from the grooves and from nanotube interior, which

occurs at the highest temperature (Figure 2).

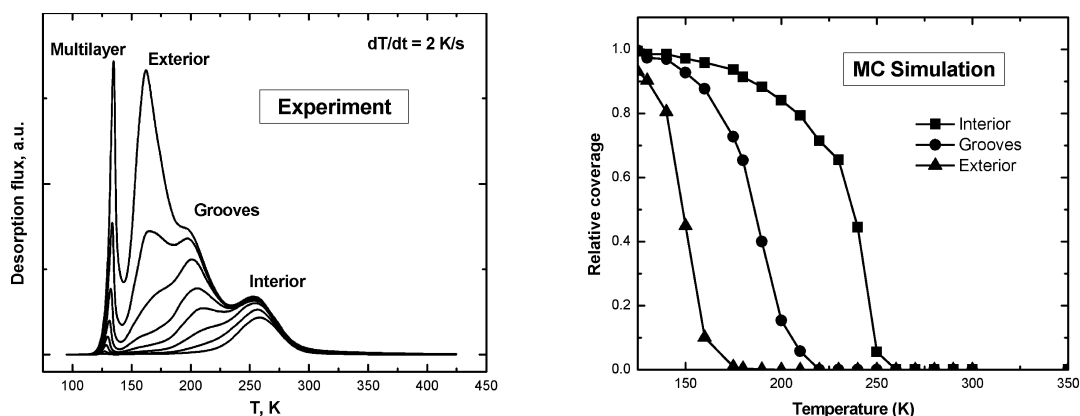


Figure 2. Temperature-programmed desorption (TPD) of *n*-pentane for increasing exposures (left) and an MC simulation of the desorption process from three types of adsorption sites (right). The derivatives of the data from the simulation correspond approximately to the peaks in the experimental spectra on the left. On the basis of the comparison between the simulation and experiment, the assignment of the TPD peaks can be made. Reprinted with permission from Ref 7. Copyright 2005 American Chemical Society.

iii) Determination of the energy contributions to the binding

The attractive forces involving solute, solvent, and adsorbent are responsible for molecular adsorption on CNTs, with the van der Waals force usually the dominant force that governs the adsorption onto a hydrophobic surface such as that of CNTs. Other possible interactions including hydrophobic effect, π - π bonds, hydrogen bonds and electrostatic interactions have been observed and are also responsible for the adsorption of molecules on CNT surface.¹⁰ These interactions, their strengths and contribution to the overall adsorption are a function of the properties of both molecules and CNTs and are often difficult to quantify experimentally. We recently used MM-PBSA calculations to decompose the energy contributions of the binding energy of lysozyme to CNTs.¹¹ This kind of analysis allows the full comprehension of the physical nature of the adsorption process and offers the possibility to design adsorbents with improved performance.

iv) *MD simulations offer the possibility to understand the adsorption mechanism*

Experiments show that CNTs extract chlorinated organic contaminants from water. Their efficiency is orders of magnitude greater than that of sand, commonly used as sorbent for this kind of molecules. No clear picture was drawn from the experimental data about the mechanism of interaction of organic contaminants with CNT surfaces at the liquid-solid interface.¹² To reach the full potential benefits of CNTs in applications such as water contamination removal, a molecular level understanding of the interaction of the contaminants with CNT surfaces in the presence of water is to be reached (Figure 3).

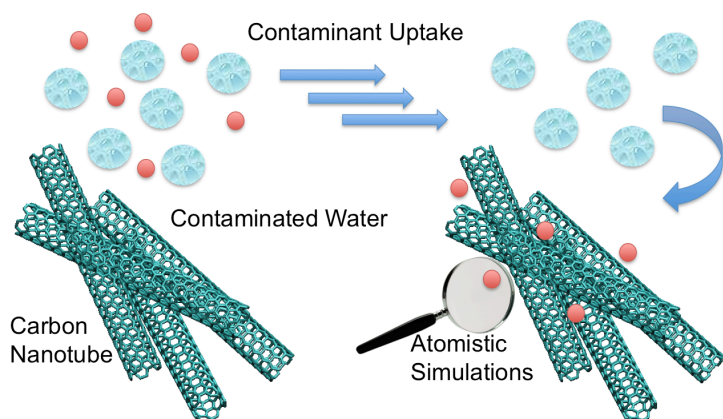


Figure 3. Atomistic simulations provide a molecular level understanding of the interaction of the water contaminants with CNT surfaces.

Molecular dynamics simulations performed on model systems emphasized the role of the hydrophobic interactions of CNT surfaces, which drive water molecules away, promoting enhanced contaminant uptake.¹²

v) *MD simulations allow system design and optimization*

The prediction of CNT optimal parameters, for instance their diameter, allows improvement of the performance of CNTs as sorbent. For example, perfluorooctanesulfonate (PFOS) is a typical persistent organic pollutant that has become of great environmental concern. The adsorption of

PFOS on CNTs of different diameters was studied with MD simulation.¹³ In the simulations, the diameters of CNTs ranged from 7.8 to 15.6 Å. The binding energy did not change monotonously with the radius. There exists an optimal diameter of CNTs for PFOS removal, which is the result of the balance between (a) the attractive forces of the molecule and the tube surface, and (b) the repulsive effect of the tube on the molecular conformation.¹³ The determination of the optimal diameter for the binding depends on the size of the adsorbate (Figure 4). In the CNTs of favourable diameter, the molecules inside the tube bind to the internal surface with the strongest non-bonding interaction and without any repulsive force. The calculation of the best pore diameter allows the optimization of the design of sorbents.

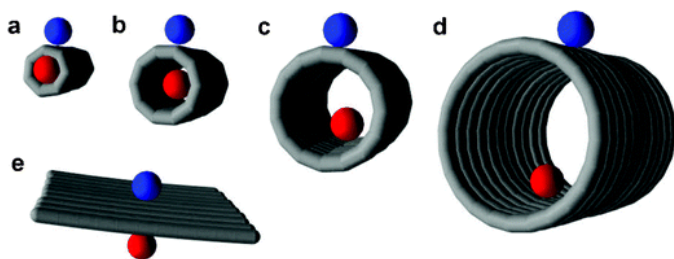


Figure 4. Endohedral and exohedral adsorption of molecules in carbon nanotubes. By varying only the diameter, the binding energy of a molecule on the nanotube changes. The outside and inside of the infinite diameter nanotube are equivalent and the binding to the exterior or interior part of the tube is the same. As the diameter decreases, the binding energy of the molecule to the exterior decreases monotonically. The ratio of guest-species diameter represented, by the red sphere, to nanotube internal diameter determines the strength of nanotube–molecule interaction. If the nanotube is too narrow, the guest species cannot be encapsulated (a); if the nanotube is too wide, the host–guest interactions are weak (c, d). A ‘snug fit’ (b) enables efficient encapsulation of the guest species inside the nanotubes. Reprinted with permission from Ref. 3 Copyright 2006 Royal Chemical Society.

CNTs for selective adsorption of molecules

CNTs, or CNTs bundles, can be used to separate binary mixtures of organic molecules and separate

hydrophobic molecules, such as H_2 , O_2 , and CO_2 gases and methane, from their aqueous solutions.¹⁴ Hydrophobic interactions between the tubes and these hydrophobic molecules drive their accumulation inside CNTs.¹⁴ Also hydrophilic molecules, such as urea, can spontaneously expel water from CNTs and accumulate inside the tube since the interactions that urea establishes with CNTs are stronger than those of water and CNTs.¹⁵

Alcohols are important products in the chemical industry. Their separation from aqueous solutions is quite difficult. Recent MD simulations observed a striking nanoscale drying phenomenon and suggested an energy-saving and efficient approach toward alcohol/water separation with CNTs.¹⁶ The simulations showed that when CNTs are immersed in aqueous alcohol solutions, even if the alcohol concentration is low (1 M), different kinds of alcohols can induce dehydration (or drying) of the nanotubes and accumulate inside both wide and narrow CNTs.¹⁶ In particular, most kinds of alcohols inside narrow CNTs form nearly uniform 1D molecular wires. For wide CNTs, the selectivity for 1-alcohols increases with the number of the alcohol carbon atoms (N_{carbon}).

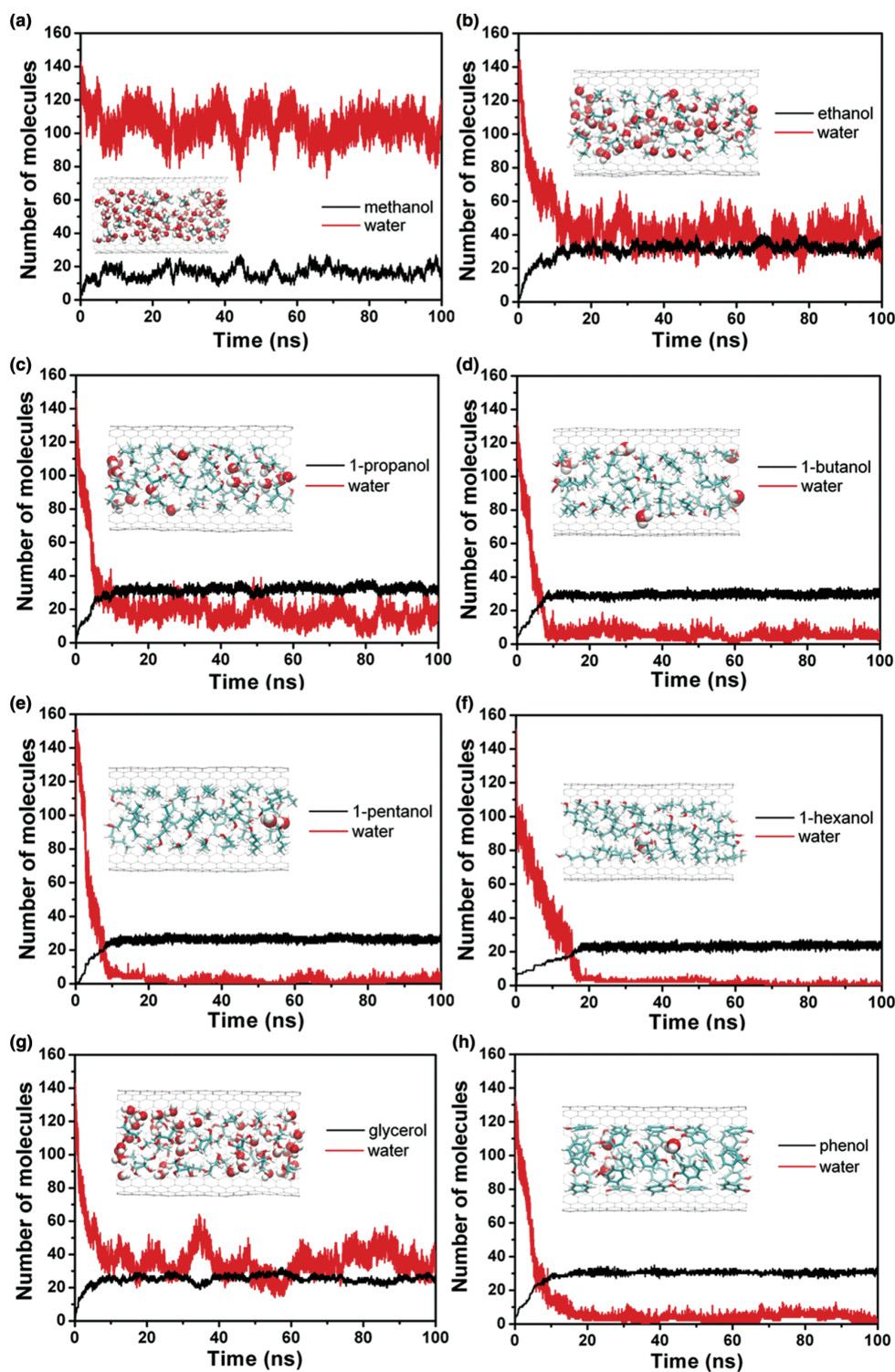


Figure 5. Number of alcohols/phenol (black line) and water molecules (red line) inside (13, 13) SWNT as a function of simulation time. Inset: Corresponding structures of the alcohols/phenol-water mixtures inside (13, 13)SWNT at equilibrium, alcohols/phenol represented by licorice and water represented by vdW spheres. Reprinted with permission from Ref 16. Copyright 2013 American Institute of Physics.

For narrow CNTs, the selectivity for 1-alcohols is very high for methanol, ethanol and propanol, and reaches a maximum when $N_{\text{carbon}} = 3$.¹⁶ These tendencies can be interpreted in terms of competition between enthalpy and entropy: for short-chain linear alcohols, the molecules inside narrow CNTs gain more vdW interaction energy compared to those inside wide CNT. As a consequence, the corresponding selectivity is larger; when $N_{\text{carbon}} > 3$, however, the entropy penalty of chains forced to be linear inside narrow SWNTs becomes significant and dominates the free energy, which results in relatively smaller selectivity compared to wide CNTs.¹⁶ This interpretation is validated by the evidence that the selectivity for phenol is much larger than selectivity for 1-hexanol inside narrow CNT.¹⁶ In short, for short-chain linear alcohols, narrow CNTs achieve the highest selectivity; while for long-chain linear alcohols, it is better to use wide CNTs to achieve efficient alcohol/water separation.¹⁶

CNTs for sensoristic applications

The electronic properties of single-walled carbon nanotubes can be altered by molecular adsorption. In general, the electronic property changes of CNTs upon exposure to molecules are attributed to the charge transfer between the molecules and the CNT. Semiconducting CNTs can be used to fabricate field-effect transistors (FETs). Chemical doping can induce strong changes in conductance.¹⁷ Such changes can be detected as current signals (Figure 6).¹⁷

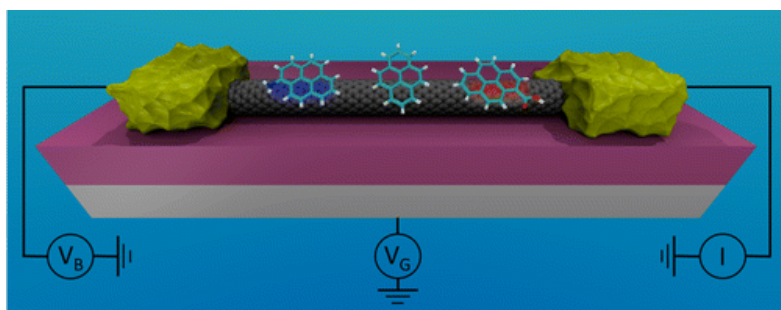


Figure 6. Inducing threshold voltage shifts of opposite sign, consistent with gating of the CNT FET by local charges. Reprinted with permission from Ref. 17. Copyright 2013 American Chemical Society.

These properties make CNTs extremely small sensors of the chemical environment. This kind of sensors is important for environmental monitoring to detect and measure the amount of specific compounds or compound classes such as pesticides, hazardous industrial chemicals, toxic metals, and pathogenic bacteria. Indeed, chemical sensors based on individual or ensembles of CNTs can detect chemicals such as NO_2 and NH_3 .¹⁸ For a semiconducting single-wall nanotube exposed to 200 ppm of NO_2 , it was found that the electrical conductance can increase by up to three orders of magnitude in a few seconds. On the other hand, exposure to 2% NH_3 caused the conductance to decrease by up to two orders of magnitude. This powerful technology is limited by the non-selective adsorption of molecules on CNTs surfaces. Rational modification of the tube surface to target specific chemical and biological analytes (covalent and supramolecular functionalization enables modification with a suite of chemical groups, metals, enzymes, antibodies, DNA molecules, and biological receptors) has allowed the development of sensors able to recognize selectively molecules, biorecognition events, (enzyme/substrate, antigen/antibody or virus recognition) and biological processes.¹⁹ In these systems, it is necessary to control i) the spatial orientation of the adsorbed molecules, or biomolecules, on the CNT surface, and ii) the conformation of the chemical moiety responsible for the recognition after adsorption (protein unfolding, for example). MD recently turned out to be an optimal tool to address these issues. Recent experiments showed that CNTs covalently functionalized with the coxsackie-adenovirus receptor (CAR) serve as biosensors capable of specifically recognizing Knob proteins from the adenovirus capsid. These experiments suggested that CAR retains its biologically active form when bound to CNT. The detailed understanding of the structural changes that occur within CAR after CNT attachment was lacking. MD showed that the CNT damps structural fluctuations in CAR and reduces the internal mobility of the protein.²⁰ The CNT induces very little structural deformation and does not affect CAR ability to bind Knob. The MD study verified that CAR retains its biological functionality when attached to CNT and provided a computational approach to rationalize the working of nanobiosensing devices.

3. PACKING

The optimal balance between binding energy and space available to accommodate molecules is the key factor governing the encapsulation and packing of molecules inside CNTs and CNTs bundles. The CNT diameter is usually the most important parameter in determining whether or not a molecule can be trapped inside a CNT. The size of the CNT cavity also controls the alignment and orientation of the molecular guests inside the tube.^{3,21,22}

CNTs application for gas storage

There is currently a strong interest in gas storage, in particular hydrogen²³⁻³² and methane³³ storage. H₂ and CH₄ are energy sources with high heat of combustion and appear to be the solution to reducing pollution and provide a realistic alternative to traditional energy sources. Despite their considerable advantages, these energy sources are not yet used extensively. The major impediments are related to the storage and transportation of these gases in a safe and economical way. CNTs are being considered as promising candidates for gas storage because of their combination of adsorption ability (high specific surface, pore microstructure, low mass density) and physical-chemical properties (chemically inert, thermally stable, mechanically strong). Gas storage is important also for other technological applications such as helium and nitrogen storage that have applications in the metallurgic industry.

Many experiments of gas adsorption in CNTs have evidenced, however, controversial results with only partial understanding of the processes. The adsorption on CNTs can be quite complex because physisorption²³⁻³¹ chemisorption³² and phenomena may coexist. Moreover, weak interactions are highly sensitive to external parameters such as temperature and pressure that may vary in different experiments. The recent scientific literature of gas adsorption in CNTs appears affected by a significant variation in the experimental data, mainly due to the different characteristics of the samples arising from the variety of the synthetic techniques used. All these aspects motivated the

use of reliable atomistic modelling to understand adsorption/desorption processes and packing of molecules inside CNTs, which are intimately related to the character and the strength of the atomistic interactions. MD simulations addressed several fundamental issues²⁵ in gas storage that included: i) the molecular distribution for a given gas load in relation to the CNT type, ii) the maximal loading (gas coverage) for a given CNT type, iii) the CNT diameter range and chirality for which gas adsorption is energetically favourable, iv) the thermodynamical and structural properties of the adsorbates after interaction with CNT / CNTs bundles, and v) the modification upon adsorption of the structure of the CNT / CNTs bundles.

Hydrogen storage is here used as an illustrative example.

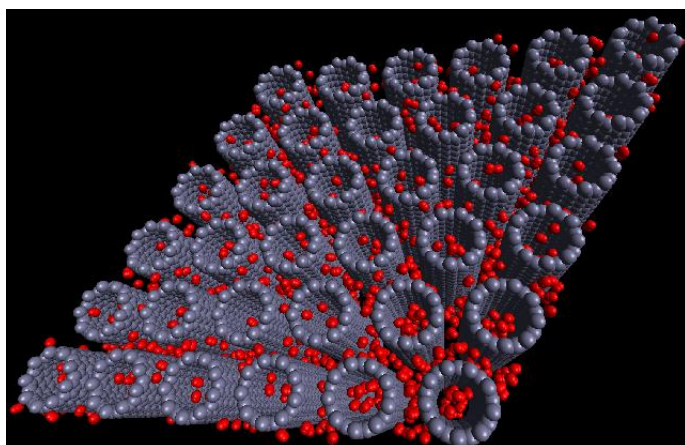


Figure 7. Hydrogen adsorption in CNTs. Hydrogen gas adsorbed in an array of (10,10) carbon nanotubes. The hydrogen inside the nanotubes and in the interstitial channels is at a much higher density than that of the bulk gas. Copyright J. Karl Johnson, University of Pittsburgh.

MD simulations investigated in detail the hydrogen molecular structures formed inside CNTs of different sizes.²⁶ In small-diameter CNTs, the significant confinement effect produced linear and helical patterns of hydrogen molecules. When a CNT of larger size is used, the hydrogen molecules formed cylindrical shells concentric with the carbon nanotube wall.²⁷ The multi-layer adsorption mechanism of H₂ was investigated also outside the tubes. Efremenko and Sheintuch evidenced the role of entropy in the adsorption process and calculated the interaction energy and entropy

associated with hydrogen adsorption on the inner and outer surfaces of CNTs of various diameters.²⁸ Adsorption energy is high in narrow nanotubes and decreases with increasing nanotube diameter.²⁸ In (8,0) nanotube, it is 3.5 times greater than on the graphite plane. The energy of adsorption on the external nanotube surfaces is lower than that for adsorption on graphite and increases with the CNT diameter.²⁸ There are no specific adsorption sites on CNTs and the diffusion is non-activated. Entropy changes are significant for hydrogen adsorption on both inner and outer nanotube surfaces, which results in a sharp increase in free energy with increasing temperature and hampers hydrogen adsorption.²⁸

For CNT bundles, initial investigations studied the effects of diameter and chirality on hydrogen storage. The results confirmed those reported for SWCNTs, showing a strong dependence on CNT diameter of hydrogen adsorption energies. The average adsorption energy increases with decreasing nanotube diameter, and there is a much smaller dependence on chirality.²⁵ The calculated average heat of adsorption for hydrogen molecules decreases as H₂ loading increases.²⁵ Analysis of the MD trajectories at the highest loading indicated that H₂ molecules form a layered structure at the endohedral sites of the larger tubes. The exohedral sites have a high density of H₂, with considerable lattice expansion. As a consequence, H₂ molecules that reside at short distance from the CNT walls interact strongly with CNT bundles and molecules at large distance from the walls experience only a very small attraction from the CNT walls, thereby reducing the average heat of adsorption. In addition, the reduction of the heat of adsorption can also be attributed partly to the large repulsive forces among H₂ molecules under compression. The average heat of adsorption decreases when H₂-H₂ repulsion is strong (at high pressure, i.e., high loading), if the H₂-CNT distance is large (at high loading and large CNT radius) and if the H₂-CNT interaction is weak (for large SWNT radius).²⁵

Weng et al.²⁹ analyzed the CNT arrays for which hydrogen adsorption is energetically favourable as a function of size, van der Waals (vdW) distance, and arrangement of carbon nanotubes. The size of

the CNT has a significant influence on the molecular distribution and the storage amount inside the CNT.²⁹ The value of the vdW distance mainly influences the hydrogen molecule distribution in the vicinity of the external wall of the carbon nanotube.²⁹ For constant distance and CNT type, the storage volumes in a square or in a triangular array lead to a difference both in volumetric and in gravimetric storage amounts.²⁹ The role of CNTs packing in bundles was underlined by Cheng *et al.* who found that for similar average CNT diameters, H₂ adsorption in inhomogeneous bundles is slightly stronger than in homogeneous bundles because the inhomogeneous bundles provide more surface area for H₂ molecules to interact with.³⁰

Investigations on CNT bundles are usually restricted to tubes having parallel axes and forming either close-packed hexagonal³⁶ or square-like⁴⁴ patterns. However, in experiments, CNTs are usually obtained as mixtures of tubes which may be intricately entangled in space. To model such structures, Seifert and coworkers³¹ considered 3-periodic arrangements of nanotubes with three and four different orientations of tube axes: Γ , $^+\Omega$, $^+\Sigma$, Σ^* (with four different orientations each), $^+\Pi$ and Π^* (with three mutually perpendicular orientations). Maximal total hydrogen uptake was found for tubes in the $^+\Sigma$ arrangement.³¹

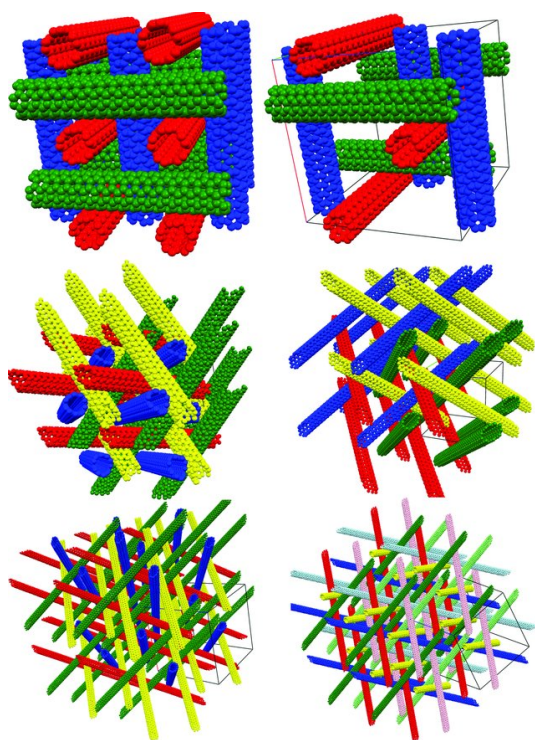


Figure 8. Different types of nanotube packings. Top left: Π^* , right: $^+\Pi$. Middle left: Γ , right: $^+\Omega$. Bottom left: $^+\Sigma$, right: Σ^* . Reprinted with permission from Ref. 31. Copyright 2011 John Wiley & Sons, Inc..

CNT for CO₂ capture and removal

Adsorption of CO₂ on carbonaceous surfaces is technologically relevant and bears on the physics of the atmosphere. The increasingly high volumes of carbon dioxide emitted in the atmosphere have stimulated interest for the development of new strategies and techniques for carbon capture and sequestration. Computational studies tried to understand, at the atomic level, the physisorption process of CO₂ on CNTs and CNT bundles. MD simulations investigating the filling of CNTs by carbon dioxide molecules showed that carbon dioxide molecules have a natural tendency to fill nanotubes and the final CO₂ concentration inside the tube can be more 100 times higher than that in the external atmosphere.³⁴ At low concentrations, carbon dioxide molecules tend to cover the internal walls of the CNT and leave almost empty the central part of the tube because CNT-CO₂ attraction is stronger than CO₂-CO₂ attraction.³⁴ Adsorption of CO₂ inside the tube depends on the internal volume of CNT. The effect of length and diameter are not similar, increasing the diameter of the tube and consequently its cross-sectional area allows an easier access to CO₂ molecules and enables a better packaging of the molecules inside the tube.³⁵ The adsorption isotherm consists of two phases, a linear and an asymptotic one. The latter corresponds to the beginning of the saturation process. As the nanotube radius increases, the transition to the asymptotic phase is delayed since nanotubes with larger internal volume and external surface require larger amounts of carbon dioxide molecules to become saturated.³⁶ Increasing CO₂ concentration causes the formation of a well defined pattern of CO₂ layers around the internal and external surfaces of the CNTs.^{34,35} The number of layers varies as a function of the nanotube diameter, size, and carbon dioxide density.³⁵

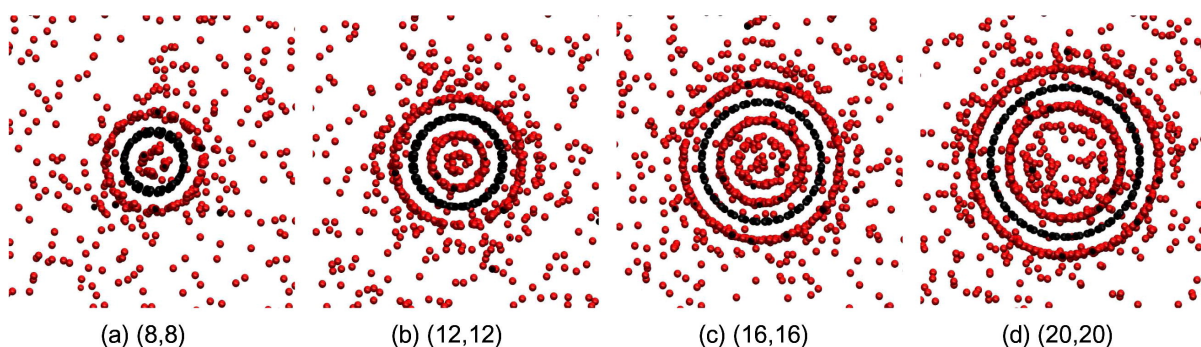


Figure 9. Projections of CO₂ distributions in (8, 8), (12, 12), (16, 16) and (20, 20) nanotubes at T= 300 K and P = 20 bar. Reprinted with permission from Ref 36. Copyright 2011, Elsevier.

At low pressures, CO₂ adsorption does not depend on the morphology of the tube. Lower values of pressure are related to lower densities and, consequently, to smaller numbers of CO₂ molecules adsorbed on the nanotube, leading to lower capacity rates. As the pressure increases above 10 bar, the density becomes sufficient to reveal the importance of nanotube surface and volume. At higher pressures, larger nanotubes present greater rates of CO₂ capture since the uptake is not restricted by the number of CO₂ molecules, but depends on the CNT available volumes. Recently, Rende et al. showed that although the amount of adsorbed CO₂ increases with increasing CO₂ concentration, the efficiency of adsorption increases with the decrease of CO₂ concentration.³⁵ Temperature is another crucial parameter to control the adsorption of CO₂ molecules in CNTs. It has a substantial impact in determining the location of CO₂ molecules both inside and around the nanotube surface.³⁵

The model of isolated CNT does not correspond to a real assembly of CNTs, especially in light of technological applications. Due to the action of attractive van der Waals forces between carbon atoms, individual CNTs self-assemble into stable bundles. This CNT arrangement creates different adsorption sites, including internal and interstitial channels, grooves, along with the rounded surface of the bundle. Kowalczyk et al.³⁷ showed that in CNT bundles both gravimetric and volumetric uptake of CO₂ strongly depend on the pore size of the nanotubes, but not on their chirality. They observed that the optimum size of the nanotube varies with the external pressure.

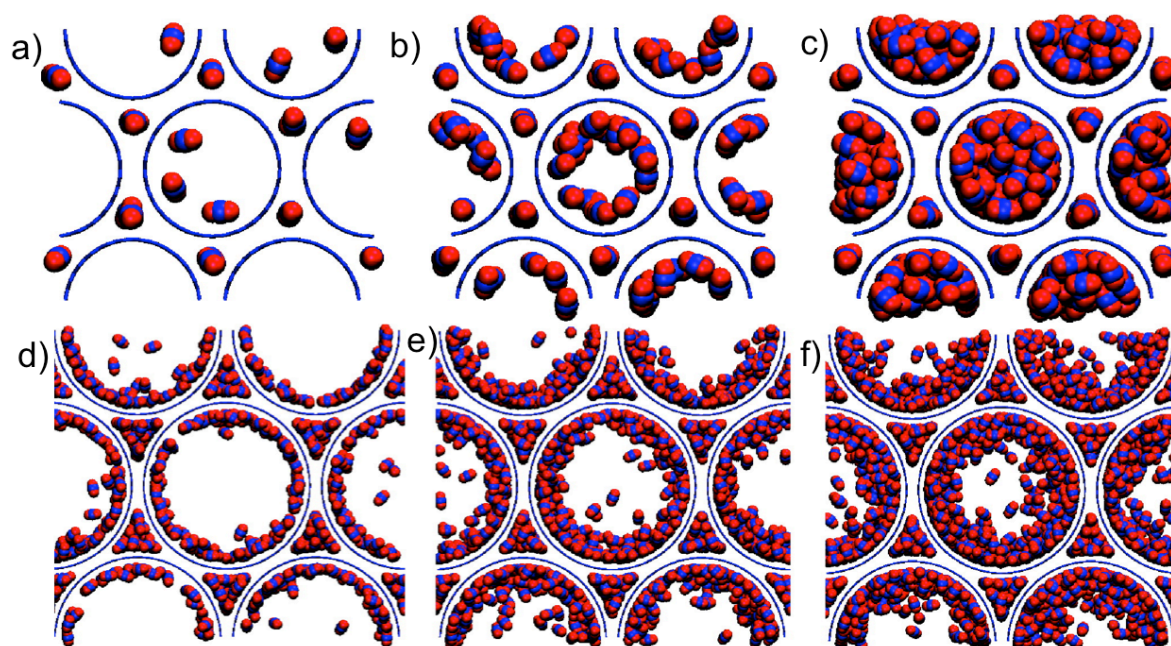


Figure 10. Snapshots of CO₂ adsorbed in a carbon nanomaterial composed of (24,0) single-walled nanotubes (equivalent pore diameter of 1.87 nm) at 298 K. The operating external pressures are (a) 0.004 MPa, (b) 0.03 MPa, (c) and 3.47 MPa. Note that CO₂ adsorbed in interstitial channels between cylindrical carbon pores form quasi-one-dimensional dense structures stabilized by strong solid–fluid interactions. Snapshots of CO₂ adsorbed in a carbon nanomaterial composed of (60,0) single-walled nanotubes (equivalent pore diameter of 4.66 nm) at 298 K. The operating external pressures are (d) 0.15 MPa, (e) 0.53 MPa, and (f) 1.32 MPa. Note the multilayer formation and growth of adsorbed CO₂ layers in internal cylindrical carbon pores. Reprinted with permission from 37. Copyright 2010 American Chemical Society.

Recently, the effect of intertube distance on the adsorption isotherm and isosteric heat of adsorption was addressed.³⁷ The selectivity of CO₂ adsorption varies with different intertube distances. At small intertube distances ($d \leq 0.5$ nm), the adsorption sequence includes i) grooves and inner surface, ii) interstitial region, iii) inner region. For $d > 0.5$ nm, it changes to: i) inner surface adsorption and partial outer surface adsorption, ii) complete outer surface adsorption, iii) interstitial, groove and inner regions.³⁸

4. FLUXES

In CNTs a number of unusual diffusional effects have been observed. They have no counterpart in bulk phases because of the interaction between molecules and the walls/surfaces.³⁹ Molecules can flow through CNTs faster than what predicted by conventional fluid-flow theory.⁴⁰⁻⁴² The high fluid velocity results from an almost frictionless interface with the carbon-nanotube wall.^{41,42} The rapid transport of molecules through CNTs is primarily due to the absence of any corrugation in the molecule-CNT potential energy surface.⁴¹ As a consequence, the slip length inside the nanotubes increases dramatically.⁴² This phenomenon provides the opportunity to perform important chemical separations with minimal use of energy. Since the diffusional properties of guest molecules in CNTs is quite sensitive to small differences of host structures, CNTs have been widely used in membrane technology. When the length scale of the system is down to a few nanometers, fluidodynamics Navier-Stokes equations are no longer accurate. The flow is mainly affected by the movements of the discrete particles that compose the system at the atomic level.⁴³ At this scale, MD is the most effective way to describe the details of the flow and to address nanofluidics issues. Two approaches in MD have been widely used to study CNT-based membranes: equilibrium and non-equilibrium molecular dynamics (NEMD) simulations.⁴⁴ Although equilibrium MD obtains time correlation functions, NEMD is more efficient for obtaining transport coefficients and for determining shear and bulk viscosity, thermal conductivity, and diffusion coefficients. The properties that can be calculated by MD and NEMD in membrane based processes have been recently reviewed.⁴⁵ Indeed, molecular level modelling has come to be a critical tool for obtaining a better understanding of molecular separation by CNTs. Understanding the behaviour of water confined in CNTs is of foremost importance, since nano-confined water presents unusual properties that differ from both the bulk liquid and gas phases.³⁹

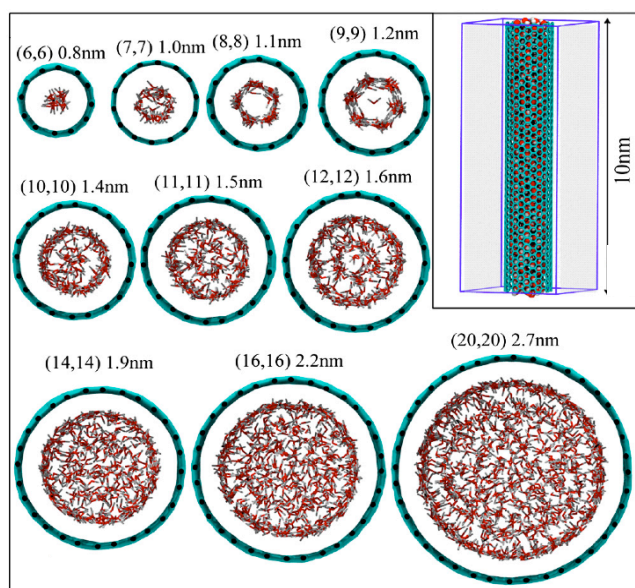


Figure 11. Structure of water molecules inside carbon nanotubes of varying diameters. Reprinted with permission from Ref 39. Copyright 2011, National Academy of Sciences.

The interplay between confinement and hydrophobicity induces modifications in the structural and dynamical properties of water.³⁵ CNTs with nanometre-scale diameters, for instance, support water flow rates that exceed the expectations of macroscopic hydrodynamics by orders of magnitude.³⁶ It has been argued that water molecules literally fly through the carbon nanotubes without touching the hydrophobic walls, hence their reduced friction and enhanced transport rates.

In the following, the focus will be on specific applications where MD simulations provided principles for the optimization and design of technological systems based on CNT-based membranes.

Ion Selective Membrane

In their pioneering work, Peter and Hummer, comparing hydrophobic pores of CNTs to similar biological ion channels, observed in MD simulations that narrow non-polar pores (less than 5 Å in diameter) blocked Na⁺ ions. Slightly wider pores (10 Å diameter) were highly permeable to the ions.⁴⁶ In order to penetrate the narrow pores, ions must strip their solvation shell, which entails a

large energy penalty; in the wider pores, the first shell remains intact, and the penalty for translocation reduces essentially to the entropic loss for confining an ion in a pore.

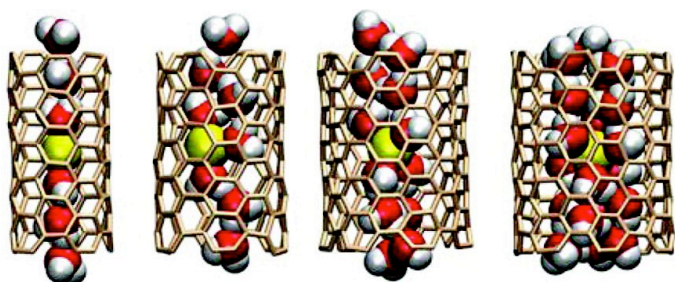


Figure 12. Snapshots from molecular dynamics simulations showing the configuration of water coordinating a sodium ion in (5,5), (6,6), (7,7), and (8,8) CNTs. In narrow nanotubes, very few water molecules coordinate the permeating ion (sodium in yellow). In wider nanotubes (right), water coordination is more bulk-like, resulting in a smaller energy barrier for ion transport.

Reprinted with permission from Ref. 54. Copyright 2008, American Chemical Society.

The same pores block completely Cl^- ions permeation, because of their larger size.⁴⁶ Liu et al. showed that a membrane of CNT (10,0) (4.4 Å diameter) selects K^+ against Na^+ : the key to ion selectivity rests on the characteristics of the hydrated ion, and the corresponding energy of partial desolvation.⁴⁷ Song and Corry tried to explain the observed selectivity revealing that Na^+ , K^+ , and Cl^- encounter different free energy barriers when entering CNT.⁴⁸ As before, most of the differences result from the different dehydration energies of the ions; the authors determined how changes in the solvation shell structure inside the nanotube and how van der Waals interactions in the smaller tubes play a significant role. Lu and coworkers⁴⁹ focused on the hydration of Na^+ and K^+ in infinitely long CNTs. Simulations indicated that inside the CNTs the preferential orientation of water molecules in the coordination shells of these two cations presents an anomalous variation and produces a diameter-dependent interactions between the cation and water molecules.⁴⁹

Comparing the results for five different CNTs, it was found that hydrated K^+ is best confined inside

the two narrow CNTs with diameters of 6.0 and 7.3 Å. The situation differs for Na⁺ ions that favour CNTs with diameters of 8.7, 10.0, and 12.8 Å.⁴⁹ These results may appear odd since the size of K⁺ is greater than that of Na⁺. However, they resemble what happens in Nature, where Na⁺-selective protein channels are generally wider than K⁺-selective channels. Energy barriers for desolvation do not correlate with pore size; instead, there were distinct regimes related to dehydration.⁵⁰ Ion transport is greatly hindered when the effective pore radius is smaller than the hydrated radius.⁵⁰ Small energy barriers are still observed when pore sizes are larger than the hydrated radius due to the re-orientation of the hydration shell or the loss of water molecules of the second shell of hydration.⁵⁰ MD simulation overcome the major limitation of current nano-filtration computer models where hydration is not present.

i) *Separation of different types of ions in water*

When considering ion separation by CNTs, the challenge for separating ions such as Na⁺ and K⁺ is particularly strong since they carry the same +1e charge and are of similar size. In the study of ion selectivity, it was found that (10,0) and (11,0) CNTs favour the passage of K⁺ over Na⁺. The investigation also determined the temperature and pressure conditions that allow Na⁺ to percolate.⁴⁷ Corey et al. carried out MD simulations under hydrostatic pressure using CNT with radii varying from 3.4 to 6.1 Å. They showed that CNT membranes can act as ion sieves, with the pore radius and pressure determining which ions permeate through the membrane.⁴⁸ Kim et al. investigated the importance of inter-ion dependence and confirmed that careful design can lead to the practical separation of sodium and potassium using diameter variation alone.⁵¹ Very recently, MD simulations examined also the energetics of Li⁺ and Mg²⁺ translocation in a variety of different CNTs and the potential use of CNTs as ion sieves for their separation. The global demand for Li-ion battery keeps growing and separation of lithium and magnesium has increasingly become the focus of many researches. The potential of mean force for ion translocation showed that Mg²⁺ ions face a greater energy barrier than Li⁺ ions when passing CNTs with same diameter. The free energy

difference of ~ 8 kJ/mol seems to be the threshold to effectively separate Li^+ and Mg^{2+} . By cautiously choosing the CNT size and the pressure across the membrane, Li^+ can be extracted from the bulk.⁵²

ii) *Seawater desalination*

The most common method of desalination, namely “reverse osmosis”, involves the use of semi-permeable membranes to filter out dissolved salts and fine solids. High pressure, and thus significant energy, is required to force water through the membranes. The cost of supplying this energy is one of the major impediments to the wide scale use of seawater desalination systems. A mechanism for alleviating these costs is to develop nanoporous semi-permeable membranes containing continuous channels that can pass greater volumes of water for a given pressure, while still blocking the passage of ions. In Nature there exist biological water pores, known as aquaporins, that are able to pass rapidly water and to block ions. The salt rejection properties of conveniently selected CNTs, and the extremely high flow rate of water inside these nanochannels, suggested the potential use of CNTs as desalination systems. Kalra et al. studied osmosis through a membrane made of carbon nanotubes by way of molecular dynamics (MD) simulation.⁵³ Corry demonstrated the potential effectiveness of nanotubes in achieving significant osmosis for application in desalination technologies.⁵⁴

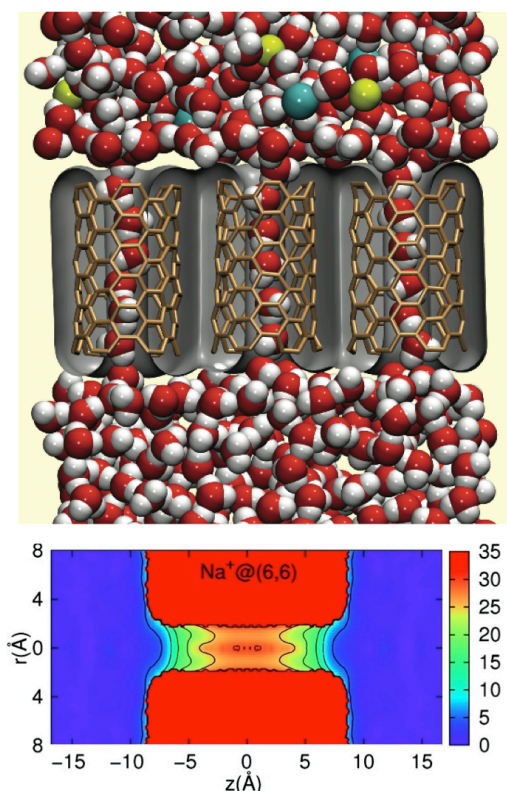


Figure 13. (Top) An array of carbon nanotubes is highly permeable to water, but not sodium (yellow) and chloride (green) ions. Reprinted with permission from Ref 54. Copyright 2008, American Chemical Society. (Bottom) Two-dimensional PMF profiles for Na^+ in (6,6) SWNT system. A barrier of $29.8 \text{ kcal mol}^{-1}$ is calculated for Na^+ permeation. A similar barrier ($29.0 \text{ kcal mol}^{-1}$) is calculated for Cl^- permeation. Reprinted with permission from Ref 48. Copyright 2009 American Chemical Society.

By calculating the potential of mean force for ion and water translocation, he showed that ions face a large energy barrier and will not pass through the narrow (5,5) and (6,6) armchair tubes. Water, however, faces no such impediment due to the formation of stable hydrogen bonds and crosses the tubes with very large rates. By measuring this conduction rate under a hydrostatic pressure difference, the author showed that membranes incorporating CNTs can, in principle, achieve a high

degree of desalination at flow rates far in excess of existing membranes.⁵⁴ More recently, Jia et al. investigated the possibility to use CNTs also in forward osmosis for the desalination process.⁵⁵

iii) *Removal of drinking water contaminants by nano-filtration*

Understanding the principles underlying the transport or the rejection of ions is of particular interest for improving filtration techniques. The transport of anionic drinking water contaminants (fluoride, chloride, nitrate and nitrite) through narrow pores, with effective radii from 2.5 to 6.5 Å, was systematically evaluated using molecular dynamics simulations to elucidate the magnitude and origin of energy barriers encountered in nanofiltration.⁵⁶ Free energy profiles for ion transport through the pores showed that the barriers depend on pore size and ion properties and that there are three key regimes: i) The first regime occurs when the ion fits in the pore with its full inner hydration shell; it is characterized by relatively small energy barriers due to rearrangement of the inner hydration shell and/or displacement of further hydration shells; ii) The second regime occurs when the pore size is between the bare ion and the hydrated ion; the energy barriers are larger due to partial dehydration of the ions; iii) The third regime occurs when the ion size approaches that of the pore, in this case the pore becomes too small for bare ions to fit regardless of hydration and thus energy barriers are extremely high, and permeation is forbidden.⁵⁶ Careful tailoring of the pore properties may enable these dehydration barriers to be harnessed to improve the rejection of anionic contaminants in nanofiltration and thus can contribute to future membrane models and design.

Gas separation

The separation of gases is crucial in a variety of processes, including many of industrial interest. CNTs offer the possibility of improving selectivity/permeability since they exhibit significantly higher fluxes than other membrane materials, as was first shown by Skoulidas et al. using molecular dynamics simulations.⁴¹ Gas separation technologies based on CNTs exploit differences in the relative capture/penetration rates of the gas components in the CNTs and/or relative diffusion rates

of the gas components inside them.⁵⁷ In size sieving, only gases smaller than the CNT pore can permeate whereas larger gas molecules are excluded. When the CNT pore size becomes much larger than both gas molecules that are going to be separated, differential chemical affinity, i.e. adsorption energies, can be exploited as sieving mechanism.

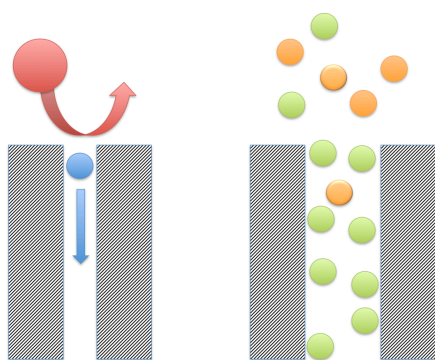


Figure 14. (Left) Size sieving; blue and red spheres represent gas molecules with small and large diameters able, or not, to enter inside the CNT. (Right) Chemical affinity sieving; green and orange spheres represent gases with stronger and weaker adsorption on the carbon nanotube inner surface.

Size Sieving

An extensively investigated example of size sieving is H₂ purification. H₂ diameter presents a significant difference in molecular diameter compared to other undesirable gases such as CO₂, CH₄, and CO that often accompany hydrogen in industrial steam methane reforming. A straightforward way to separate H₂ is to use a specifically designed molecular sieve with high selectivity and permeability. The key factor in utilizing the size exclusion effect for gas separation is to select CNTs with appropriate pore width. A (5,5)CNT bundle behaves as a perfect molecular sieve for separation of hydrogen from methane. The tube diameter is ~ 6.8 Å, and the interstitial channels of this membrane are too small to accommodate methane molecules. The smaller hydrogen molecules can be adsorbed in the internal and interstitial channels between the nanotubes.⁵⁸ In the interior of

(5,5)CNTs adsorbed/compressed hydrogen forms a quasi-one-dimensional crystal. Porous carbon nanotubes, which are single-wall carbon nanotubes with tailored pores in their sidewalls, were proposed also as potential membrane materials for separating gas mixtures with high selectivity and high permeability.^{59,60}

Chemical Affinity Sieving

Separation mechanisms for gas diffusion through CNTs occur also when the pore size is larger than that of both types of molecules: the component with the stronger chemical affinity with the CNT is adsorbed on the wall surface, while the component with lower interaction is not. The mechanism therefore relies on the preferential uptake of one of the gas components. Sholl et al. showed that a (10,10)CNT is highly selective for methane over hydrogen. The explanation rests in the much stronger interactions of CH₄ with the graphitic tube walls.⁶¹ At very high pressures, the adsorption selectivity decreases. This generic behaviour is typical of mixtures where the weaker adsorbing species has a larger saturation capacity than the more strongly adsorbing species.⁶¹

Considering bundles of CNTs of different diameters, the selectivity greatly depends on the diameter of the CNT.⁵⁸ Pores that can accommodate layers of methane molecules give the optimum pore width for the separation of methane molecules.⁶² At low loadings, energy is the only important parameters, when loading increases other parameters have to be considered such as entropy, diffusion properties, etc.^{63,64} For example, studies of the selective adsorption in CNTs of N₂/O₂ under different pressures, showed that at low loading, N₂ is preferentially adsorbed; however, at high loadings O₂ becomes the larger component due to entropic effects.

5. PERSPECTIVE / CONCLUSION AND OUTLOOK

The discussion presented here shows that atomistic simulations can provide a molecular level description and understanding of adsorption, packing and flux phenomena involved in the technological applications of CNTs. There are still many open questions to be addressed and solved

and new and uncharted roads to explore in the use of computer simulations. To name a few:

i) *Modeling CNTs*. Standard force fields (Amber,⁶⁵ Charmm,⁶⁶ Gromos,⁶⁷ OPLS-AA,⁶⁸ UFF,⁶⁹ CVFF,⁷⁰ etc.) are used to model the CNTs, even if in many simulations this approach is sufficiently accurate, peculiar mechanical properties of the tube, that can play an important role, such as elasticity, deformation, etc. may not be accurately described. There are few simulation that use the more computationally expensive reactive potentials such as the Tersoff or the Brenner Potentials,⁷¹ the Reactive Empirical Bond Order (REBO),⁷² the AIREBO⁷³ and the ReaxFF,⁷⁴ which can provide this kind of description. Little or no allowance is made for the metallic nature of the CNTs.

ii) *Molecule-CNT interactions*. Most of the MD studies of CNTs use van der Waals parameters from generic force fields. Hummer showed that the physical picture of a process depends on the details of Lennard-Jones parameters used in the simulation.⁷⁵ When these parameters are used outside the parameterization region where they were conceived (for example parameters developed to simulate proteins and not generic molecules), they should be carefully tested⁷⁶ and/or recalibrated.⁷⁷

iii) *CNT Polarizability*. Due to their delocalized π -electrons, CNTs are highly polarizable. Sometimes the effect of the polarization of the nanotube is negligible or provide very small contributes to the total interaction energy,⁷⁸ sometimes neglecting the polarization of CNTs can strongly affect the description of the adsorption, packing and transport properties of molecules in CNTs.⁷⁹

iv) *Virtuous "Recycling" of well-tested methodologies*. Recently, we used methodologies developed in the drug design field, to study CNT/(bio)molecule interactions. Docking may provide a very fast protocol to determine the best geometry of adsorption of molecules. This approach was tested and validated with different nano-objects.^{11,80-82} Analogously, free energy methods used for drug discovery (MM-PBSA, LIE, Free Energy Perturbation, Thermodynamic Integration) to determine

the binding of drugs to receptors, can estimate quickly and precisely the ΔG of binding between molecules and CNT and, more importantly, provide information that is inaccessible experimentally, but of primary importance to design optimized systems.¹¹ There is a lot of computational protocols that can be exported from the pharmaceutical field to find new application in molecule/CNT interactions.

v) *QM/MM*. Molecular mechanics simulations, even if they can provide a realistic description of many processes, cannot describe the CNTs electronic properties that in some circumstances are fundamental to understand the system under examination.^{83,84} The hybrid QM/MM (quantum mechanics/molecular mechanics) approach combines the strengths of the QM (accuracy and electronic description of the system) and MM (computational speed) approaches.^{83,84}

vi) *Upscaling atomistic simulations*. Mesoscale simulations⁸⁵ and continuum models⁸⁶ forfeit the atomistic description of the CNTs, but may provide an accurate description of the mechanical, electrical, thermal and fluidodynamic performance of CNT for engineering applications of CNT-based devices. Connections between the different time and length scales are currently achieved either by parameterization or by ‘coarse-graining’ procedures.⁸⁵ Alternatively, atomistic simulations can be used to obtain input data to insert directly in the analytical expression typical of continuum modeling.⁸⁶ In this way, the fluid-dynamical behavior of a CNT-based membrane, the mechanical performance of a CNT-based gas storage system, or the peculiar properties of a CNT-reinforced composite can be obtained from bottom up.

vii) *Need for experimental validation of simulation results*. Bridging experiments, models and simulations is necessary. Until now atomistic simulations have been used only to provide molecular-level description of the phenomena under investigation and to afford a clearer interpretation of experimental data. A truly integrated approach should create a virtuous cycle able to the design specific experiments to test and validate the results of the simulations. The validation

process establishes the accuracy of the model and/or simulations. Validation provides a crucial piece of evidence to support models or simulations credibility for a particular application and increases its predictive power.

REFERENCES

1. M. F. L. De Volder, S. H. Tawfick, R. H. Baughman and A. J. Hart, *Science*, 2013, **339**, 535.
2. P. Knodratyuk and J. T. Yates, Jr., *Acc. Chem. Res.*, 2007, **40**, 995.
3. D. A. Britz and A. N. Khlobystov, *Chem. Soc. Rev.*, 2006, **35**, 637.
4. J. K. Holt, *Adv. Mater.*, 2009, **21**, 3542.
5. M. S. Mauter and M. Elimelech, *Environ. Sci. Technol.*, 2008, **42**, 5843.
6. B. Pan and B. Xing, *Environ. Sci. Technol.*, 2008, **42**, 9005.
7. P. Knodratyuk, Y. Wang, J. K. Johnson and J. T. Yates, Jr., *J. Phys. Chem. B*, 2005, **109**, 20999
8. O. Byl, P. Knodratyuk, S. T. Forth, S. A. Fitzgerald, L. Chen, J. K. Johnson and John T. Yates, Jr., *J. Am. Chem. Soc.*, 2003, **125**, 5889.
9. M. R. LaBrosse, W. Shi and J. K. Johnson, *Langmuir*, 2008, **24**, 9430.
10. K. Yang and B. Xing, *Chem. Rev.*, 2010, **110**, 5989.
11. M. Calvaresi, S. Hoefinger and F. Zerbetto, *Chem. Eur. J.*, 2012, **18**, 4308.
12. X. Ma, D. Anand, X. Zhang, M. Tsige and S. Talapatra, *Nano Res.*, 2010, **3**, 412.
13. Y. Li, J. Niu, Z. Shen and C. Feng, *Chemosphere*, 2013, **91**, 784.
14. J. Lee and N. R. Aluru, *Appl. Phys. Lett.*, 2010, **96**, 133108.
15. P. Das and R. Zhou, *J. Phys. Chem. B*, 2010, **114**, 5427.
16. X. Tian, Z. Yang, B. Zhou, P. Xiu and Y. Tu, *J. Chem. Phys.*, **2013**, 138, 204711.

17. M. B. Lerner, J. M. Reszczenski, A. Amin, R. R. Johnson, J. I. Goldsmith, and A. T. C. Johnson, *J. Am. Chem. Soc.*, 2012, **134**, 14318.
18. J. Kong, N. R. Franklin, C. Zhou, M. G. Chapline, S. Peng, K. Cho and H. Dai, *Science*, 2000, **287**, 622. 2000, 287, 1801.
19. M. Calvaresi and F. Zerbetto, *Acc. Chem. Res.*, 2013, **46**, 2454.
20. R. R. Johnson, B. Jon Rego, A. T. C. Johnson and M. L. Klein, *J. Phys. Chem. B*, 2009, **113**, 11589.
21. W. Plank, R. Pfeiffer, C. Schaman, H. Kuzmany, M. Calvaresi, F. Zerbetto and J. Meyer, *ACS Nano*, 2010, **4**, 4515.
22. X. Liu, H. Kuzmany, P. Ayala, M. Calvaresi, F. Zerbetto and T. Pichler, *Adv. Funct. Mat.*, 2012, **22**, 3202.
23. G. E. Froudakis *Mater. Today*, 2011, **14**, 324
24. Y Xia, Z. Yang and Y. Zhu, *J. Mater. Chem. A*, 2013, **1**, 9365.
25. H. Cheng, A. C. Cooper, G. P. Pez, M. K. Kostov, P. Piotrowski and S. J. Stuart, *J. Phys. Chem. B*, 2005, **109**, 3780.
26. Y. Ma, Y. Xia, M. Zhao and M. Ying, *Chem. Phys. Lett.*, 2002, **357**, 97.
27. L. Guo, C. Ma, S. Wang, H. Ma and X. Li, *J. Mater. Sci. Technol.*, 2005, **21**, 123.
28. I. Efremenko and M. Sheintuch, *Langmuir*, 2005, **21**, 6282.
29. C.-I Weng, S.-P. Ju, K.-C. Fang and F.-P. Chang, *Comp. Mater. Sci.*, 2007, **40**, 300.
30. M. T. Knippenberg, S. J. Stuart and H. Cheng, *J. Mol. Model*, 2008, **14**, 343.

31. B. Assfour, S. Leoni, G. Seifert and I. A. Baburin, *Adv. Mater.*, 2011, **23**, 1237.
32. S. K. H. An, Y. H. Lee, G. Seifert and T. Frauenheim, *J. Am. Chem. Soc.*, 2001, **123**, 5059.
33. O. O. Adisa, B. J. Cox and J. M. Hill, *Nanoscale*, 2012, **4**, 3295.
34. A. Alexiadis and S. Kassinos, *Chem. Phys. Lett.*, 2008, **460**, 512.
35. D. Rende, L. Ozgur, N. Baysal and R. Ozisik, *J. Comput. Theor. Nanosci.*, 2012, **9**, 1658.
36. D. Mantzalis, N. Asproulis and D. Drikakis, *Chem. Phys. Lett.*, 2011, **506**, 81.
37. P. Kowalczyk, S. Furmaniak, P. A. Gauden and A. P. Terzyk, *J. Phys. Chem. C*, 2010, **114**, 21465.
38. M. Rahimi, J. K. Singh, D. J. Babu, Jo. J. Schneider and F. Müller-Plathe, *J. Phys. Chem. C*, 2013, **117**, 13492.
39. T. A. Pascal, W. A. Goddard and Y. Jung, *Proc. Natl. Acad. Sci. USA* 2011, **108**, 11794.
40. J. H. Walther, K. Ritos, E. R. Cruz-Chu, C. M. Megaridis and P. Koumoutsakos, *Nano Lett.*, 2013, **13**, 1910.
41. A. I. Skoulidas, D. M. Ackerman, J. K. Johnson and D. S. Sholl, *Phys. Rev. Lett.*, 2002, **89**, 185901.
42. M. Majumder, N. Chopra, R. Andrews and B. J. Hinds, *Nature*, 2005, **438**, 44.
43. H. Verweij, M. C. Schillo and J. Li, *Small*, 2007, **3**, 1996
44. F. Zhu, E. Tajkhorshid, and K. Schulten, *Phys. Rev. Lett.*, 2004, **93**, 224501.
45. H. Ebro, Y. M. Kim and J. H. Kim, *J. Membr. Sci.*, 2013, **438**, 112.

46. C. Peter and G. Hummer, *Biophys. J.*, 2005, **89**, 2222.
47. H. Liu, C. J. Jameson and S. Murad, *Mol. Simulat.*, 2008, **34**, 169.
48. C. Song and B. Corry, *J. Phys. Chem. B*, 2009, **113**, 7642.
49. Q. Shao, J. Zhou, L. Lu, X. Lu, Y. Zhu and S. Jiang, *Nano Lett.*, 2009, **9**, 989.
50. L. A. Richards, A. I. Schäfer, B. S. Richards and B. Corry, *Small*, 2012, **8**, 1701.
51. J. J. Cannon, D. Tang, N. Hur and D. Kim, *J. Phys. Chem. B*, 2010, **114**, 12252.
52. D. Yang, Q. Liu, H. Li and C. Gao, *J. Membr. Sci.*, 2013, **444**, 327.
53. A. Kalra, S. Garde and G. Hummer, *Proc. Natl. Acad. Sci. U.S.A.*, 2003, **100**, 10175.
54. B. Corry, *J. Phys. Chem. B*, 2008, **112**, 1427.
55. Y. Jiaa, H. Lia, M. Wanga, L. Wua and Y. Hu, *Sep. Purif. Technol.*, 2010, **75**, 55.
56. L. A. Richards, A. I. Schafer, B. S. Richardsa and B. Corry, *Phys. Chem. Chem. Phys.*, 2012, **14**, 11633.
57. Y. Jiao, A. Du, M. Hankela and S. C. Smith, *Phys. Chem. Chem. Phys.*, 2013, **15**, 4832.
58. P. Kowalczyk, L. Brualla, A. Zywockinski and S. K. Bhatia, *J. Phys. Chem. C*, 2007, **111**, 5250.
59. B. J. Bucior, D.-L. Chen, J. Liu and J. K. Johnson, *J. Phys. Chem. C*, 2012, **116**, 25904.
60. H. Liu, V. R. Cooper, S. Dai and D. E. Jiang, *J. Phys. Chem. Lett.*, 2012, **3**, 3343.
61. H. Chen and D. S. Sholl, *J. Membr. Sci.*, 2006, **269**, 152.
62. K. V. Kumar, E. A. Muller and F. Rodríguez-Reinoso, *J. Phys. Chem. C*, 2012, **116**, 11820.

63. J. Jiang and S. I. Sandler, *Langmuir*, 2004, **20**, 10910.
64. G. Arora and S. I. Sandler, *J. Chem. Phys.*, 2005, **123**, 044705.
65. W. D. Cornell, P. Cieplak, C. I. Bayly, I. R. Gould, K. M. Merz Jr, D. M. Ferguson, D. C. Spellmeyer, T. Fox, J. W. Caldwell and P. A. Kollman, *J. Am. Chem. Soc.*, 1995, **117**, 5179.
66. A: D. MacKerell Jr., D. Bashford, M. Bellott, R. L. Dunbrack Jr., J. D. Evanseck, M. J. Field, S. Fischer, J. Gao, H. Guo, S. Ha, D. Joseph-McCarthy, L. Kuchnir, K. Kuczera, F. T. K. Lau, C. Mattos, S. Michnick, T. Ngo, D. T. Nguyen, B. Prodhom, W. E. Reiher III, B. Roux, M. Schlenkrich, J. C. Smith, R. Stote, J. Straub, M. Watanabe, J. Wiorkiewicz-Kuczera, D. Yin and M. Karplus, *J. Phys. Chem. B*, 1998, **102**, 3586.
67. C. Oostenbrink, A. Villa, A. E. Mark and W. van Gunsteren, *J. Comput. Chem.*, 2004, **25**, 1656.
68. W. L. Jorgensen, D. S. Maxwell and J. Tirado-Rives, *J. Am. Chem. Soc.*, 1996, **118**, 11225.
69. A. K. Rappe, C. J. Casewit, K. S. Colwell, W. A. Goddard III and W. M. Skiff, *J. Am. Chem. Soc.*, 1992, **114**, 10024.
70. P. Dauber-Osguthorpe, V. A. Roberts, D. J. Osguthorpe, J. Wolff, M. Genest and A. T. Hagler, *Proteins*, 1988, **4**, 31.
71. D. W. Brenner, *Phys. Rev. B*, 1990, **42**, 9458.
72. D. W. Brenner, O. A. Shenderova, J. A. Harrison, S. J. Stuart, B. Ni and S. B. Sinnott, *J. Phys.: Condens. Matter*, 2002, **14**, 783.
73. S. J. Stuart, A. B. Tutein and J. A. Harrison, *J. Chem. Phys.*, 2000, **112**, 6472.
74. A. C. T. van Duin, S. Dasgupta, F. Lorant and W. A. Goddard III, *J. Phys. Chem. A*, 2001, **105**, 9396.

75. G. Hummer, J. Rasaiah and J. Noworyta, *Nature*, 2001, **414**, 188.
76. B. Shi, G. Zuo, P. Xiu and R. Zhou, *J. Phys. Chem. B*, 2013, **117**, 3541.
77. Y. Wu and N. R. Aluru, *J. Phys. Chem. B*, 2013, **117**, 8802.
78. F. Moulin, M. Devel and S. Picaud, *Phys. Rev. B*, 2005, **71**, 165401.
79. D. Lu, Y. Li, S. V. Rotkin, U. Ravaioli and K. Schulten, *Nano Letters*, 2004, **4**, 2383.
80. M. Calvaresi and F. Zerbetto, *ACS Nano*, 2010, **4**, 2283.
81. M. Calvaresi and F. Zerbetto, *Nanoscale*, 2011, **3**, 2873.
82. M. Calvaresi and F. Zerbetto, *J. Chem. Inf. Model.*, 2011, **51**, 1882.
83. G. E. Froudakis, *Nano Lett.*, 2001, **1**, 179
84. P. Giacinto, A. Bottoni, M. Calvaresi and F. Zerbetto, *J. Phys Chem. C*, 2014, **118**, 5032.
85. M. Calvaresi, M. Dallavalle and F. Zerbetto, *Small*, 2009, **5**, 2191.
86. Y. L. Chen, B. Liu, J. Wu, Y. Huang, H. Jiang and K. C. Hwang, *J. Mech. Phys. Solids*, 2008, **56**, 3224.